A local segmentation parameter optimization approach for mapping heterogeneous urban environments using VHR imagery

Tais Grippa*[a], Stefanos Georganos[a], Moritz Lennert[a], Sabine Vanhuysse[a], Eleonore Wolff[a]
[a] Department of Geosciences Environment and Society - Institute for Environmental Management and Land-use Planning (DGES-IGEAT), Université libre de Bruxelles, Belgium

ABSTRACT

Mapping large heterogeneous urban areas using object-based image analysis (OBIA) remains challenging, especially with respect to the segmentation process. This could be explained both by the complex arrangement of heterogeneous land-cover classes and by the high diversity of urban patterns which can be encountered throughout the scene. In this context, using a single segmentation parameter to obtain satisfying segmentation results for the whole scene can be impossible. Nonetheless, it is possible to subdivide the whole city into smaller local zones, rather homogeneous according to their urban pattern. These zones can then be used to optimize the segmentation parameter locally, instead of using the whole image or a single representative spatial subset. This paper assesses the contribution of a local approach for the optimization of segmentation parameter compared to a global approach. Ouagadougou, located in sub-Saharan Africa, is used as case studies. First, the whole scene is segmented using a single globally optimized segmentation parameter. Second, the city is subdivided into 283 local zones, homogeneous in terms of building size and building density. Each local zone is then segmented using a locally optimized segmentation parameter. Unsupervised segmentation parameter optimization (USPO), relying on an optimization function which tends to maximize both intra-object homogeneity and inter-object heterogeneity, is used to select the segmentation parameter automatically for both approaches. Finally, a land-use/land-cover classification is performed using the Random Forest (RF) classifier. The results reveal that the local approach outperforms the global one, especially by limiting confusions between buildings and their bare-soil neighbors.

Keywords: Object Based Image Analysis, Unsupervised Segmentation Parameters Optimization, Local Approach, Urban Area, Land Cover Mapping

1. INTRODUCTION

Land-use/land-cover (LULC) maps are essential decision-making tools as they can provide a picture of the current urban configuration, enabling the deployment of appropriate policies for urban planning and management. This is especially true in the sub-Saharan African urban context where cities undergo high growth rates and decision makers usually face the scarcity of reference information.

Nowadays, the availability of very-high-resolution (VHR) remote sensing (RS) imagery is higher than ever. This allows for unprecedented capabilities for the production of spatially and thematically detailed LULC maps. VHR RS data enable mapping a large diversity of elements of the urban landscape, such as buildings, roads or trees. However, the production of such detailed maps still remains a challenging task and requires the use of appropriate image analysis techniques in order to achieve accurate results. The processing of VHR RS imagery is usually performed using object-based image analysis (OBIA) techniques. While pixel-based techniques classify each pixel individually, OBIA groups similar pixels into segments (objects)[1] and classifies those new geographical entities. OBIA has been shown to outperform pixel-based analyses in several studies[2], due to the elimination of the so-called 'salt and paper' effect and the utilization of geometrical and contextual features.

This document is the authors version of the paper submitted to Proc. SPIE 10431, Remote Sensing Technologies and Applications in Urban Environments II, ; doi: 10.1117/12.2278422; http://dx.doi.org/10.1117/12.2278422 and available on www.spiedigitallibrary.org

Several studies[3–6] showed that the quality of the segmentation has an impact, even if not straightforward[4], on the accuracy of the final classified map and requires therefore a particular attention. Assessing the quality of the segmentation results can be achieved in a supervised way, either by visual interpretation of the segments, or by comparing these to a reference segmentation layer. Unfortunately, these approaches are time-consuming and subjective[7]. Recently, new techniques have appeared to enable the assessment of segmentation results in an unsupervised way[8–12]. Using these techniques, it is therefore possible to automate the selection of the segmentation parameter. These so-called 'unsupervised segmentation parameter optimization' (USPO) techniques mainly seek to maximize intra-segment homogeneity and inter-segment heterogeneity[7]. Their main advantage that they operate on a purely unsupervised manner, as they rely on metrics computed directly on the data, and usually produce results comparable to those of supervised methods[13].

Most of the time, when the area of interest is very large, both supervised and unsupervised optimization approaches are performed on a representative spatial subset, i.e., a limited portion of the whole scene, in order to reduce computational costs which can be a major issue. Although this approach may be acceptable for homogeneous areas, it would be rather unintuitive to assume that a single parameter, even optimized, can adequately segment different landscape patterns throughout large heterogeneous areas such as sub-Saharan African cities. In fact, it would be more reasonable to make the assumption that the optimal segmentation parameter can differ across the scene. As such, by using a single – global - parameter, the segmentation results may potentially add an unnecessary bias into the segmentation algorithm by forcing a single value for the whole image, while the most optimal parameter is likely to vary for different urban patterns.

In recent years, a few studies have tackled this issue, by employing more localized or regionalized optimization procedures. Cánovas-García and Alonso-Sarría (2015) demonstrated an improvement in segmentation quality by optimizing the segmentation parameter based on spatially differentiated agricultural plots, instead of selecting a single parameter for the whole scene[14]. Recently, Kavzoglu et al. (2016) proposed a regionalized multiscale approach in which an initial coarse segmentation was carried out in order to produce areas for further refinement of the segmentation parameters[15]. Classification results were shown to improve when the optimization of the segmentation parameter was performed regionally rather than globally. To our knowledge, no studies have tackled this issue in heterogeneous urban environments.

In this paper, we present a framework for investigating the contribution of a local segmentation parameter optimization approach compared to a global approach. The area of interest, located in the city of Ouagadougou in Burkina Faso, covers 94 square kilometers (km²) and is highly heterogeneous in terms of urban patterns. Firstly, a global approach was performed in which the whole scene was segmented based on a single parameter selected by USPO on a spatial subset representative of the diversity of the whole scene. Secondly, a local approach was carried out using a partition of the city into 283 local zones, homogeneous in terms of building size and building density. Each local zone was then segmented using a locally optimized segmentation parameter. The whole framework was based on an open source semi-automated processing chain[16].

The research presented in this paper is part of the 'Modeling and forecasting African Urban Population Patterns for vulnerability and health assessments' project (MAUPP – http://maupp.ulb.ac.be), focusing on production of LULC maps and estimations of human population densities in African cities.

2. MATERIAL AND METHODS

2.1 Processing chain, software and tools

The analysis was performed using the open-source software GRASS GIS[17] and R. The segmentation step was performed using 'i.segment' and 'i.segment.uspo' from GRASS GIS and the classification step using the 'caret' package of R. The whole processing was coded in Python and embedded in a 'Jupyter notebook'[18]. Python was used in order to chain commands of GRASS GIS and R directly in the same interface, and in a similar fashion as the chain presented in a previous publication[16] and publicly available.

This document is the authors version of the paper submitted to Proc. SPIE 10431, Remote Sensing Technologies and Applications in Urban Environments II, ; doi: 10.1117/12.2278422; http://dx.doi.org/10.1117/12.2278422 and available on www.spiedigitallibrary.org

2.2 Data

The dataset consists of a pan-sharpened stereo WorldView-3 imagery, with visible and near-infrared (VNIR) bands, re-sampled by the provider to a spatial resolution of 0.5 m. It was acquired during the wet season (October 2015) in order to enhance the spectral separability between bare soils and artificial surfaces. A normalized digital surface model (nDSM) was produced by photogrammetry from the WorldView-3 stereo-pairs and was used to provide height information. Additional indices were computed from the VNIR bands, i.e., the normalized vegetation index (NDVI), the normalized water index (NDWI)[19] and the Spectral Shape Index (SSI)[20]; they were used during the classification step.

2.3 Case study

We applied the analysis to a subset of the city of Ouagadougou in Burkina Faso. The city has been undergoing an extensive urban sprawl during the last decades and the number of inhabitants has doubled between 2004 and 2014 according to the United Nations[21]. It covered an area of around 615 km² at the time of imagery acquisition in 2015. The subset dedicated to the analysis is located northeast to the city center (see Figure 1) and covers 94 km². The extent of the AOI is very large compared to other studies and according to the spatial resolution of the data[22].

The city of Ouagadougou is an interesting case study for assessing the contribution of a locally optimized segmentation parameter approach as it is composed of highly contrasted neighborhoods in terms of urban patterns (see Figure 2).

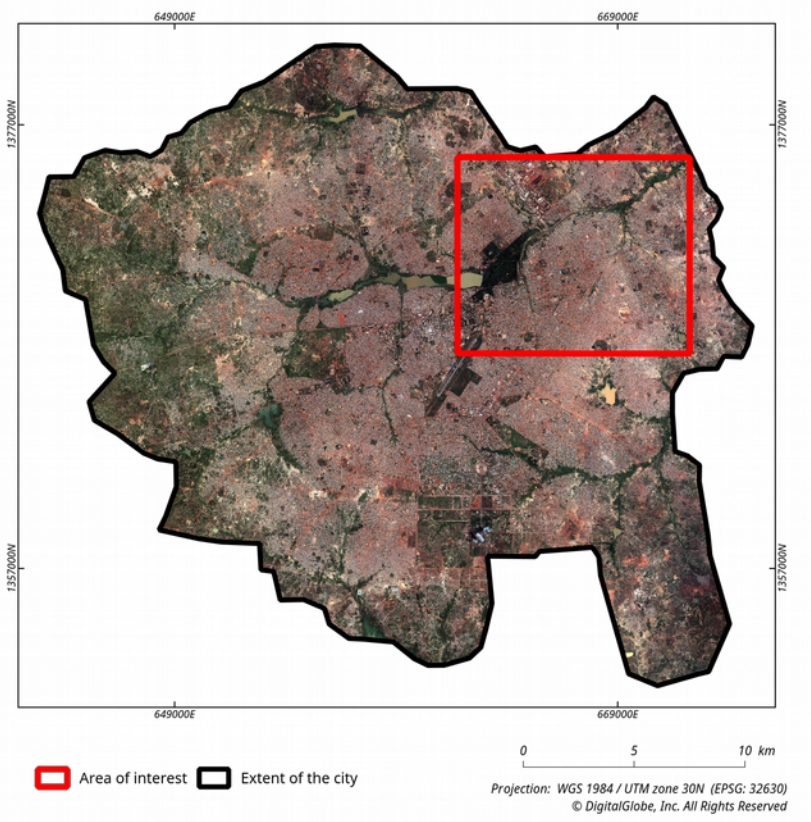

Figure 1: Extent of the city of Ouagadougou, Burkina Faso, and footprint of the area of interest used in this research.

This document is the authors version of the paper submitted to Proc. SPIE 10431, Remote Sensing Technologies and Applications in Urban Environments II, ; doi: 10.1117/12.2278422; http://dx.doi.org/10.1117/12.2278422 and available on www.spiedigitallibrary.org

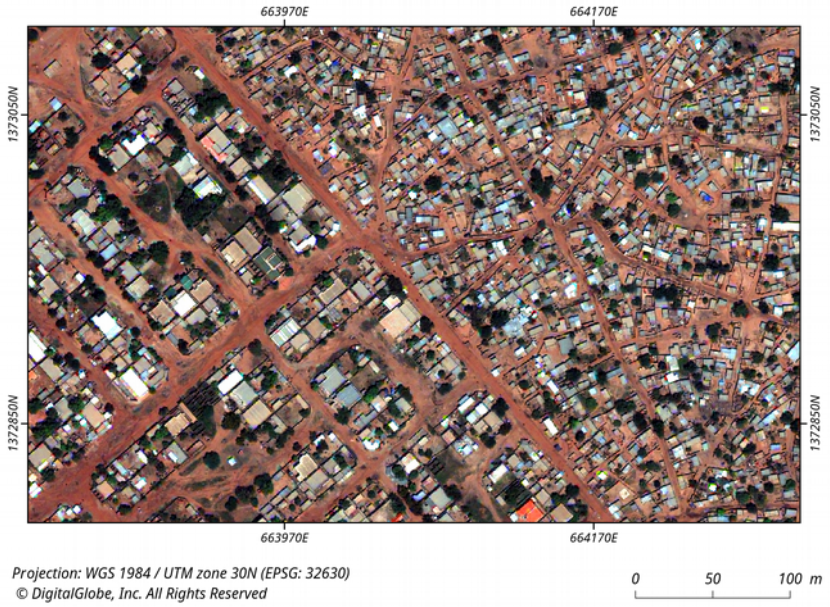

Figure 2: Subset of the area of interest with a clear opposition between unplanned and planned residential neighborhoods, with varying building sizes and densities.

2.4 Segmentation and Unsupervised Segmentation Parameter Optimization (USPO)

Segmentation is a very important step in an OBIA classification workflow. Indeed, the segmentation quality can affect the accuracy of the classification. In this paper, an unsupervised segmentation parameter optimization (USPO) method is used in order to automate the selection of the optimum segmentation parameter. The main advantage of such method is that it relies on 'goodness measures'[7] quantifying the desired characteristics a good segmentation should have, i.e., homogeneous objects which are different from their neighbors.

In this paper we used the 'i.segment' module of GRASS GIS software to perform the segmentation. The latter implements a region-growing segmentation algorithm which is ruled by two parameters. The main parameter is the 'threshold' which controls the tolerance for merging contiguous objects according to their proximity in the feature space. The second parameter is the 'minsize' which controls the minimum size of segments. It is implemented at the end of the segmentation process, and merges the objects that are too small with their most similar neighbors.

In GRASS GIS, unsupervised segmentation parameter optimization is possible using the 'i.segment.uspo' add-on. The latter was used in this study to automatically select the optimum threshold parameter. The minsize parameter was fixed in order to match the desired minimum mapping unit of the final map, i.e., 3.75 m². The add-on allows users to select different USPO approaches presented in previous studies[8,12] and its implementation is described in Grippa et al. (2017)[16]. It generates a stack of different segmentation results by varying the threshold parameter and selects the one that obtains the largest score for an optimization function. The score combines a measure of intra-object weighted variance (WV)[23] assessing the intra-segment homogeneity and a spatial autocorrelation (SA) measure assessing the inter-segment heterogeneity. For the SA measure, the user can choose between Geary's C[24] and Moran's I[25]. The latter was used in this paper. Both measures are normalized using the following function[8]:

$$WV_{norm} = \frac{WV_{Max} - WV}{WV_{Max} - WV_{Min}} \quad (1)$$

and

$$SA_{norm} = \frac{SA_{Max} - SA}{SA_{Max} - SA_{Min}} \quad (2)$$

Where WV is the weighted variance and SA is the spatial autocorrelation measure of the current segmentation

This document is the authors version of the paper submitted to Proc. SPIE 10431, Remote Sensing Technologies and Applications in Urban Environments II, ; doi: 10.1117/12.2278422; http://dx.doi.org/10.1117/12.2278422 and available on www.spiedigitallibrary.org

layer. WV_{Max} , WV_{Min} and SA_{Max} , SA_{Min} refer respectively to the maximum and minimum WV and SA value in the stack of segmentation.

The normalized measures are then combined using the F-function proposed by Johnson (2015)[12] which is computed as follows :

$$F=(1+\alpha^2)\times\frac{SA_{norm}\times WV_{norm}}{\alpha^2\times SA_{norm}+WV_{norm}} \quad (3)$$

Where F is an 'overall goodness' measure, ranging from 0 (poor quality) to 1 (high quality). The segmentation result that reaches the highest value of F is then selected as the optimum one. The α parameter can be used to modify the importance of SA_{norm} in the optimization function. In our case this parameter was fixed to 1.

Recent research revealed that the overall goodness measure resulting from this USPO approach is highly dependent on the range of parameter considered during the optimization procedure[26]. Therefore, we performed some empirical tests to find parameters generating clearly over-segmented and under-segmented results. The range was fixed as starting at a threshold value of 0.004 and stopping at 0.030, using a incremental step of 0.001.

2.5 Segmentation parameter optimization using a global approach

First, we applied a procedure that aims to select a single globally optimized segmentation parameter. We call it the 'global approach'. Due to computation time issues, the segmentation parameter optimization was not applied to the whole area of interest (AOI), but to a limited subset. This design is frequently used when dealing with very large datasets and was applied in previous research[12]. We made sure that the selected spatial subset contains all the types of urban patterns which can be found in the whole scene (see Figure 3). This spatial subset covers more than 10% of the whole AOI (10.2 km² / 94 km²).

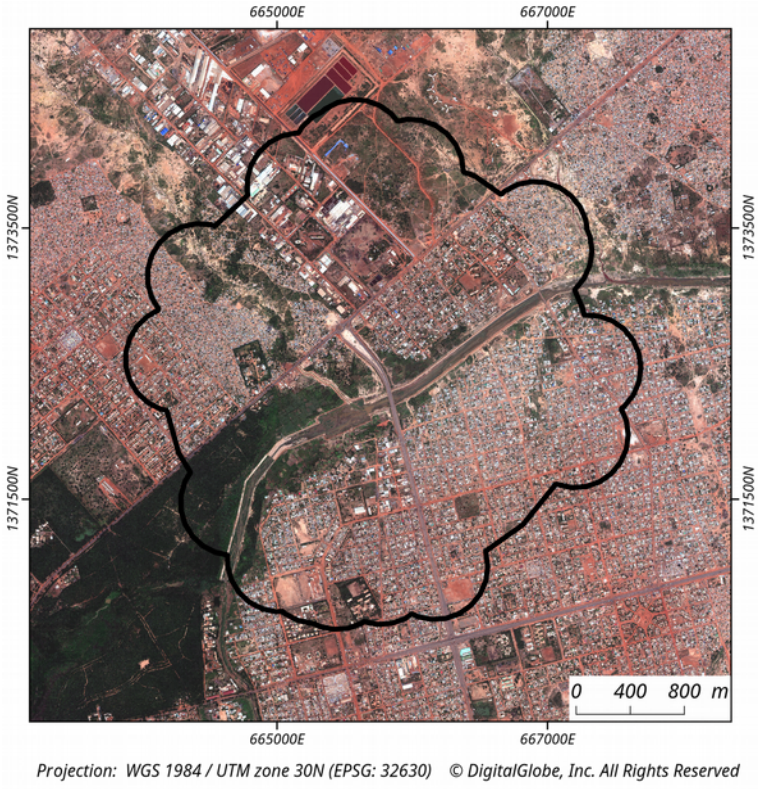

Figure 3: Spatial subset used for the global optimization of segmentation parameter. The subset covers more than 10% of the whole AOI and is representative of the diversity of urban patterns which can be found in the scene.

This document is the authors version of the paper submitted to Proc. SPIE 10431, Remote Sensing Technologies and Applications in Urban Environments II, ; doi: 10.1117/12.2278422; http://dx.doi.org/10.1117/12.2278422 and available on www.spiedigitallibrary.org

In this global approach, the segmentation parameter optimization was applied to the spatial subset, using the i.segment.uspo GRASS GIS add-on. The suggested threshold is assumed to be optimal for the whole scene. The latter was then segmented with the i.segment GRASS GIS module, using this globally-optimized threshold.

2.6 Segmentation parameter optimization using a local approach

Next, we applied a procedure in order to optimize the segmentation parameter for different 'local zones' (LZs) of the AOI. The reason for applying this procedure, named the 'local approach', is that the AOI presents a very high heterogeneity in terms of urban patterns (see Figure 2). Therefore, we assumed that segmenting different parts of the city using locally optimized segmentation parameters should enable the reduction of both over and under-segmentation, and thereby improve the quality of the final LULC map.

A partition of the area of interest in multiple zones was required in order to optimize the segmentation parameter locally. In developed countries, such reference geospatial data, e.g., city districts, street blocks or even cadastral plots, are often available. On the contrary, developing countries and especially African ones are known to suffer from a severe lack of available reference geospatial data. In the case of Ouagadougou, no preexisting reference data were available. In that context, the partition of the city into small homogeneous LZs was achieved manually, by visual interpretation based on criteria relating to building size and density. The full procedure was carried out by the same interpreter. We partitioned the AOI into multiple LZs according to the following criteria:

i. LZs should be homogenous, both in terms of building size and density, and should be visibly different from their neighboring LZs.

ii. LZs boundaries should follow, as far as possible, man-made or natural linear elements, e. g., roads, paths, rivers, streams, railways.

iii. Built-up LZs should be larger than 1.5 hectares (ha).

iv. Non-built-up LZs (vegetation, water, bare soils) should be larger than 15 ha when located in core urban areas, and larger than 20 ha when located in peri-urban areas. This criterion can be adapted on a case-by-case basis according to the situation and the judgment of the interpreter.

It should be noticed that the first two criteria are similar to those used in previous studies[27,28].

Then, we labeled LZs according to their urban morphology. For this purpose, a classification scheme combining the building sizes and density was used and named here 'morphological type'. Figures 4-5 illustrate the partition of the city into local homogenous zones and the membership of each zone to its morphological type. Snapshots of the urban pattern for some morphological type are presented on Figure 6.

This document is the authors version of the paper submitted to Proc. SPIE 10431, Remote Sensing Technologies and Applications in Urban Environments II, ; doi: 10.1117/12.2278422; http://dx.doi.org/10.1117/12.2278422 and available on www.spiedigitallibrary.org

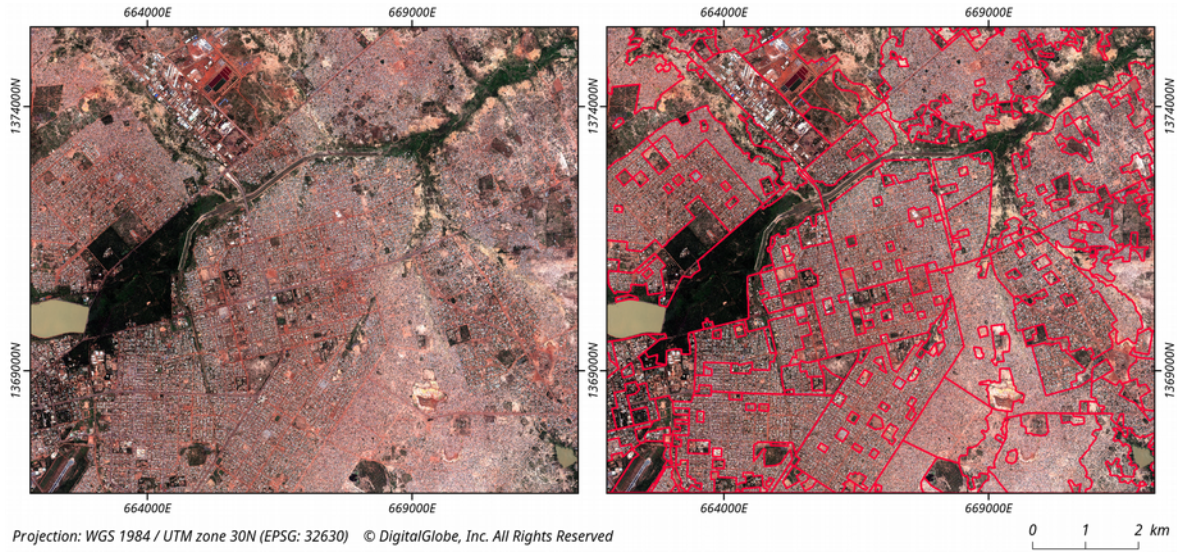

Figure 4: Partition of the city into smaller zones used for the locally optimized segmentation parameter approach.

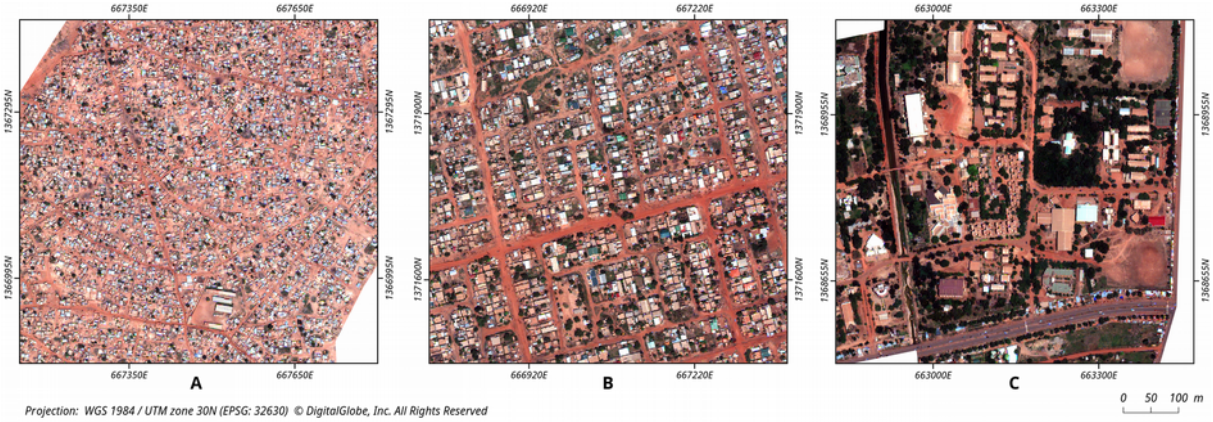

Figure 5: Examples of morphological types with different urban patterns. A) Small-sized high density built-up fabric B) Medium-sized high density built-up fabric C) Large-sized medium density built-up fabric.

This document is the authors version of the paper submitted to Proc. SPIE 10431, Remote Sensing Technologies and Applications in Urban Environments II, ; doi: 10.1117/12.2278422; http://dx.doi.org/10.1117/12.2278422 and available on www.spiedigitallibrary.org

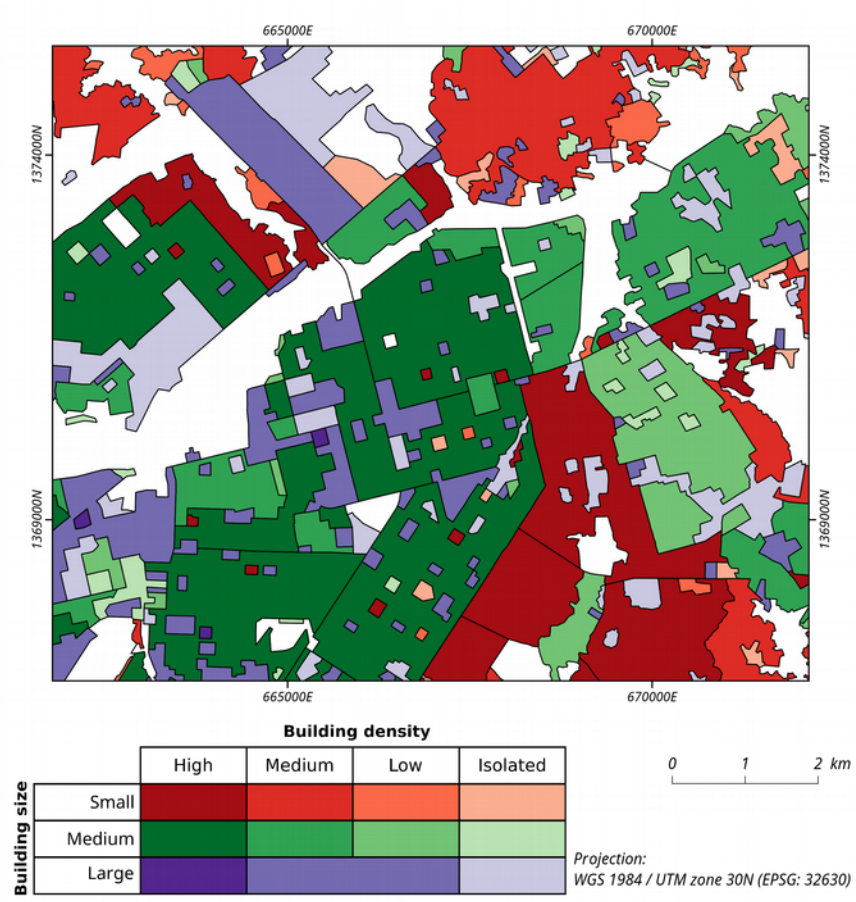

Figure 6: Membership of each local zone to its morphological type, consisting of a combination of categories of building size and density.

2.7 Legend, classification scheme and sampling

We considered 11 LULC classes in the classification scheme, as shown in Table 1. The 'caret' package of the R software was used to perform the classifications using a Random Forest (RF) classifier[29] with parameters optimized using cross validation and grid search.

The training and validation sets consisted of random samples generated automatically and labeled manually by the interpreter. In both the global and the local approach, training points were used to automatically select the segments in which they were included. A visual check of these segments was performed in order to eliminate those that mis-segmented objects and covered more than a single LULC class. This explains why small differences appear in the number of training samples for a same class (see Table 1). In total, 956 and 958 training points were used in the global and local approach, respectively. For each class of the legend, 40 points were dedicated to the validation. They were not used to train the classifier, in order to get a completely independent validation set. The validation points used to assess the classification performance of both approaches is strictly identical, allowing comparison of accuracy measures.

This document is the authors version of the paper submitted to Proc. SPIE 10431, Remote Sensing Technologies and Applications in Urban Environments II, ; doi: 10.1117/12.2278422; http://dx.doi.org/10.1117/12.2278422 and available on www.spiedigitallibrary.org

Table 1: Classification scheme and size of the training and validation sets.

Level 1 classes land cover	Level 2 classes land use/land cover	Abbreviation	Training set size global approach	Training set size local approach	Validation set size
Artificial surfaces	Buildings	BU	203	202	40
	Swimming pools	SW	72	72	40
	Asphalt surfaces	AS	63	63	40
Natural material surfaces	Brown/red bare soil	RBS	71	71	40
	White/grey bare soil	GBS	71	73	40
Vegetation	Trees	TR	95	95	40
	Mixed bare soil/vegetation	MBV	90	91	40
	Dry vegetation	DV	65	65	40
	Other vegetation	OV	77	78	40
Water	Water bodies	WB	75	72	40
Shadow	Shadow	SH	74	76	40
		Total size:	956	958	440

3. RESULTS

The results show that the values of the segmentation parameter obtained using the local optimization approach differ noticeably from those resulting from the global approach. This is consistent with the results of previous studies on local optimization of segmentation parameter[14]. Figure 7 illustrates the variation of optimized 'threshold' parameter according to the membership of the LZ to the morphological type. The first observation that can be made relates to the non-built-up zones (i.e., morphological type 0) for which the optimum segmentation parameters are mostly lower than in the global approach. On the contrary, for a large majority of built-up zones the optimized threshold is higher than in the global approach. A higher 'threshold' makes the region-growing algorithm more tolerant for merging groups of pixels, resulting in a lower number of segments in the final segmentation result.

A second observation is that the distribution of locally optimized parameters by morphological type tends to be more dispersed when the building density decreases (see Figure 7). Mapping the locally optimized segmentation parameter, as in Figure 8, confirms this non-random distribution. Also, we noticed that the smaller-sized zones get the highest values of optimized 'threshold'. The visual assessment of those smaller zones revealed that the local optimization approach achieved most of the time better segmentation and classification results. Further research should be undertaken to better understand the relationship between the size of the zones to be used for local optimization approach and the resulting segmentation and classification results.

The quantitative evaluation of the classification showed that the local optimization approach slightly outperformed the global one regarding the overall accuracy (AO). For the second level of classification, using 11 classes, the OA reached 84.77% for the global approach and 85.45% for the local one (see Table 2). These results are both satisfying considering the high number of classes and the fact that some of them are spectrally very similar, e.g., classes 'Mixed bare soil/vegetation' and 'Dry vegetation'. When considering the 5 classes of the second level, the OA reached 94.77% for the global approach and 95.45% for the local one.

This document is the authors version of the paper submitted to Proc. SPIE 10431, Remote Sensing Technologies and Applications in Urban Environments II, ; doi: 10.1117/12.2278422; http://dx.doi.org/10.1117/12.2278422 and available on www.spiedigitallibrary.org

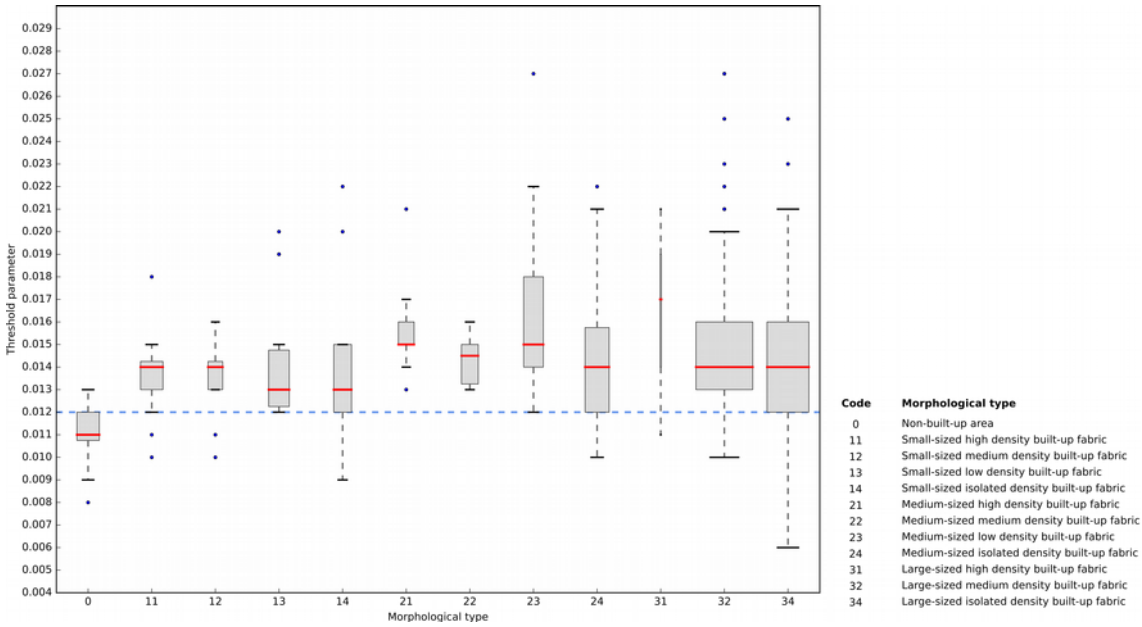

Figure 7: Boxplots representing the dispersion of locally optimized segmentation parameters by morphological type. The red lines refer to the median value. The lower and upper limits of the boxes refer to the first and third quartile, respectively. The range of the whiskers corresponds to the last observation whose value is included into 1,5 times the interquartile range. Observations with values beyond the whiskers are considered as outliers and represented by dots. The box widths are proportional to the square root[30] of the number of LZs of each morphological type. The straight dashed blue line refers to the 'threshold' derived from the global optimization approach.

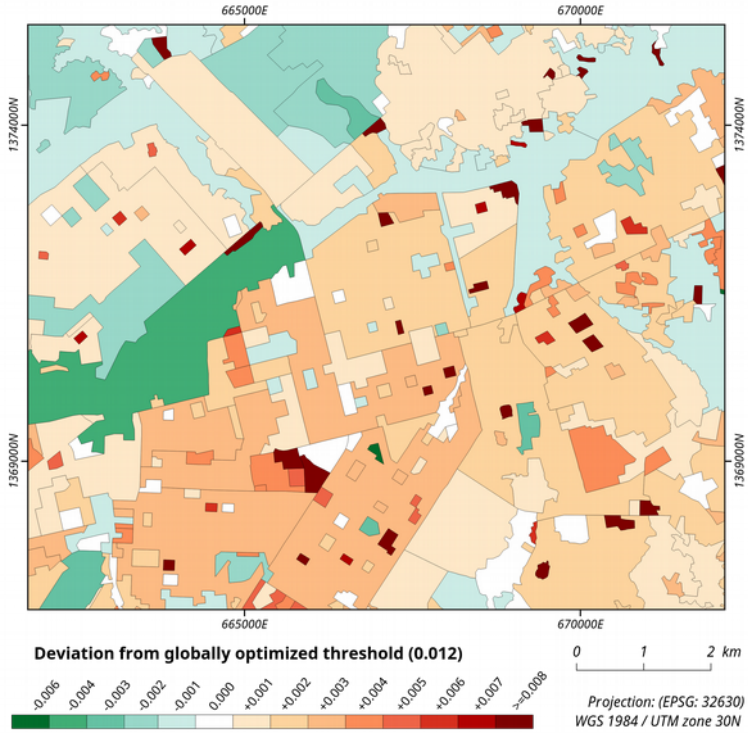

Figure 8: Spatial distribution of the locally optimized segmentation parameters. The values represent the deviation from the globally optimized segmentation parameter.

This document is the authors version of the paper submitted to Proc. SPIE 10431, Remote Sensing Technologies and Applications in Urban Environments II, ; doi: 10.1117/12.2278422; http://dx.doi.org/10.1117/12.2278422 and available on www.spiedigitallibrary.org

Table 2: Comparison of the performance evaluation of the classifications carried out using the global and the local segmentation parameter optimization approaches.

	Classification level	Overall accuracy	Kappa
Global optimization approach	L1 (5 classes)	94.77 %	0.9297
	L2 (11 classes)	84.77 %	0.8325
Local optimization approach	L1 (5 classes)	95.45 %	0.9389
	L2 (11 classes)	85.45 %	0.8400

Since the MAUPP project is mainly focused on the estimation of human population densities, the accuracy of the produced maps is particularly important with respect to the class 'Buildings'. For this reason, we mainly assessed the contribution of the local optimization approach for that specific class. The analysis of the F-score for each class of the second level of classification (see Table 3) revealed that the class 'Buildings' reaches a score of 0.92 and 0.93 using the global and the local approach, respectively. In general, the local approach achieved slightly better scores than the global one, except for the classes 'Brown/red bare soil' and 'Inland waters'.

Table 3: F-score for individual classes of the second level (L2) of the classification. For each class, if one approach outperforms the other, the F-score value is in bold.

Level 2 Classes	Global optimization approach	Local optimization approach
Buildings	0.92	**0.93**
Swimming pools	0.97	0.97
Asphalt surfaces	0.93	**0.95**
Brown/red bare soil	**0.89**	0.85
White/grey bare soil	0.85	0.85
Trees	0.81	**0.82**
Mixed bare soil/vegetation	0.69	**0.72**
Dry vegetation	0.67	0.67
Other vegetation	0.75	**0.79**
Inland waters	**0.91**	0.90
Shadow	0.95	**0.96**

Assessing the quality of the classification through quantitative performance evaluation appeared not sufficient to completely evaluate the differences appearing in the final map. Even though the classification results showed a slight OA improvement when using a local segmentation parameter optimization approach, we realized that some substantial differences occurred, especially regarding the 'Buildings' and 'Brown/red bare soils' classes. As the qualitative evaluation did not well capture some specific differences between the two approaches, we conducted a meticulous qualitative visual assessment of the classification results. Figures 9-11 present selected snapshots highlighting the main differences between the classifications resulting from both the global and the local approach.

We carefully carried out a visual analysis of the results. We discovered that, in most cases, the local segmentation optimization approach resulted in a more accurate LULC map. We can report that the most important improvement resides in the fact that the local approach better segmented bare-soil objects neighboring buildings. Those were often over-segmented using the global approach which created confusion with the 'Buildings' class. As a consequence, the local segmentation parameter optimization approach helped in limiting commission errors for the class 'Buildings'. Figures 9-10 illustrate how the delineation of buildings on the final map appears more accurate when using the local approach.

This document is the authors version of the paper submitted to Proc. SPIE 10431, Remote Sensing Technologies and Applications in Urban Environments II, ; doi: 10.1117/12.2278422; http://dx.doi.org/10.1117/12.2278422 and available on www.spiedigitallibrary.org

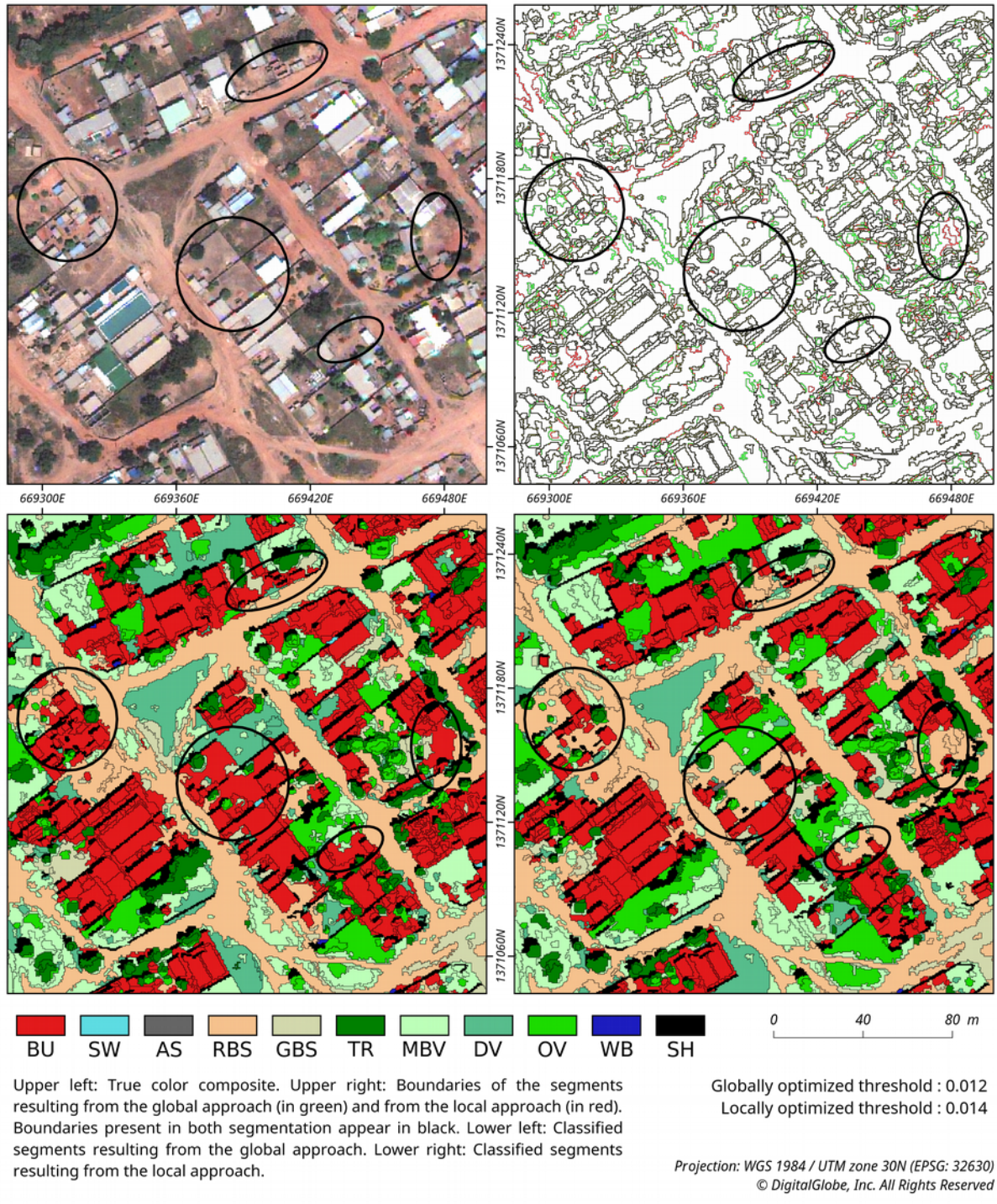

Figure 9: Subset of the AOI located in a LZ characterized by medium-sized low density built-up fabric. Bare-soil objects neighbors to the building are better classified using the local segmentation parameter optimization approach. BU: Buildings, SW: Swimming pools, AS: Asphalt surfaces, RBS: Brown/red bare soil, GBS: White/grey bare soil, TR: Tree, MBV: Mixed bare soil/vegetation, DV: Dry vegetation, OV: Other vegetation, WB: Water bodies, SH: Shadow.

This document is the authors version of the paper submitted to Proc. SPIE 10431, Remote Sensing Technologies and Applications in Urban Environments II, ; doi: 10.1117/12.2278422; http://dx.doi.org/10.1117/12.2278422 and available on www.spiedigitallibrary.org

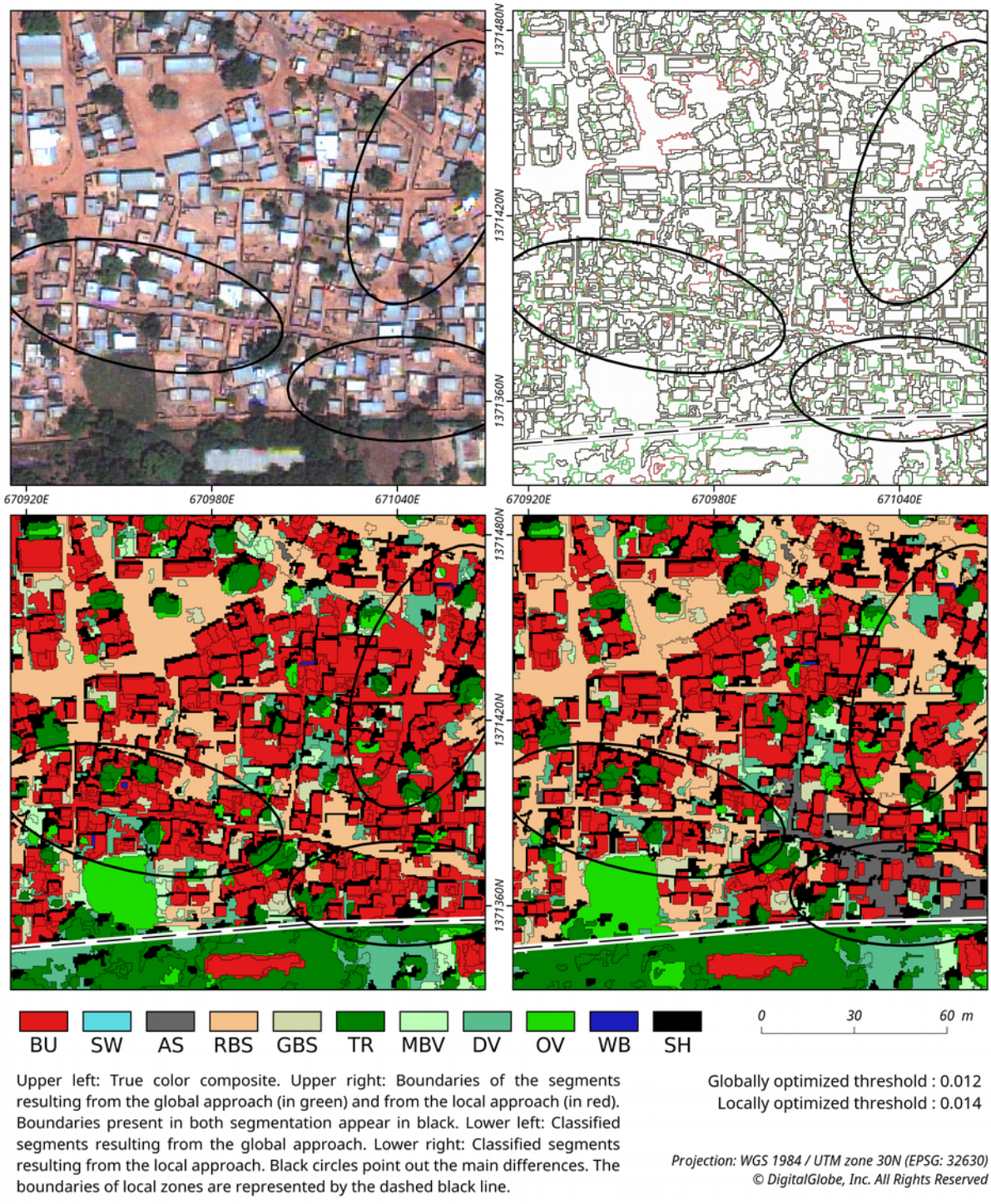

Figure 10: Subset of the AOI located in a LZ characterized by small-sized high density built-up fabric. Bare-soil objects neighbors to the building are better classified using the local segmentation parameter optimization approach. BU: Buildings, SW: Swimming pools, AS: Asphalt surfaces, RBS: Brown/red bare soil, GBS: White/grey bare soil, TR: Tree, MBV: Mixed bare soil/vegetation, DV: Dry vegetation, OV: Other vegetation, WB: Water bodies, SH: Shadow.

This document is the authors version of the paper submitted to Proc. SPIE 10431, Remote Sensing Technologies and Applications in Urban Environments II, ; doi: 10.1117/12.2278422; http://dx.doi.org/10.1117/12.2278422 and available on www.spiedigitallibrary.org

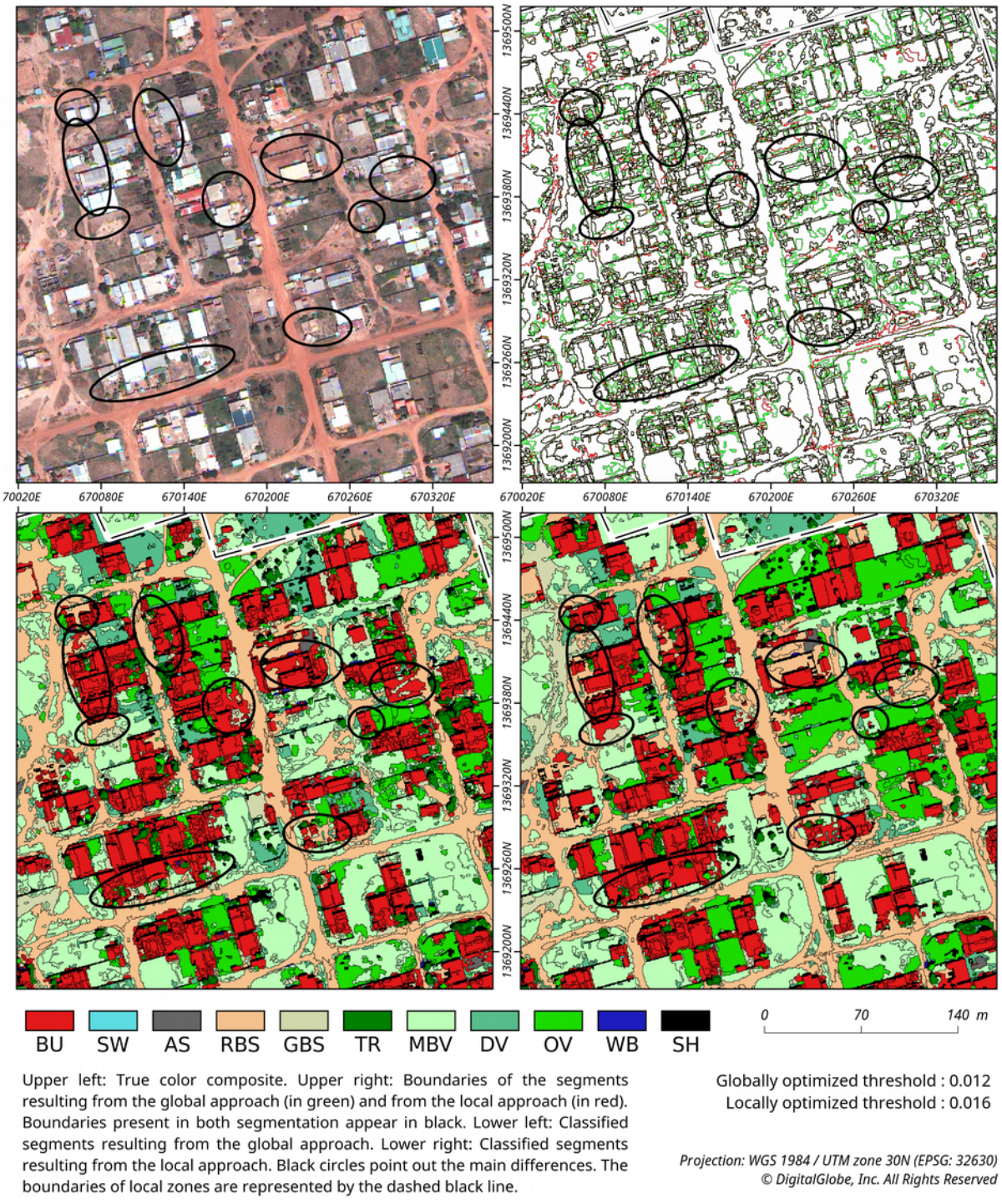

Figure 11: Subset of the AOI located in a LZ characterized by medium-sized low density built-up fabric. Here, some counter-examples illustrate the situation where local approach misclassified bare-soil objects neighboring of buildings, since the global approach accurately classified them. BU: Buildings, SW: Swimming pools, AS: Asphalt surfaces, RBS: Brown/red bare soil, GBS: White/grey bare soil, TR: Tree, MBV: Mixed bare soil/vegetation, DV: Dry vegetation, OV: Other vegetation, WB: Water bodies, SH: Shadow.

This document is the authors version of the paper submitted to Proc. SPIE 10431, Remote Sensing Technologies and Applications in Urban Environments II, ; doi: 10.1117/12.2278422; http://dx.doi.org/10.1117/12.2278422 and available on www.spiedigitallibrary.org

This confusion could be explained by the fact that the training samples for the bare-soil classes were very rarely located so close to the buildings. As such, bare-soil objects used for training were bigger and registered different feature characteristic than those over-segmented bare-soil objects neighboring buildings.

More generally, it appeared that the training set consisting of the objects created in the local approach better separated the different classes. Figure 12 illustrates the class separability in both training sets. The figure depicts the probability density function for the most important features in both RF models, i.e., the first quartile on NDVI values. It is clear that training objects of the same class are spectrally more homogeneous when using the local approach, leading to a higher intra-class homogeneity. As a consequence, the inter-class separability is higher with class centres appearing noticeably different for few classes, e.g. 'Buildings' or 'Trees'. It could also be noticed that class centres of 'Buildings' and 'Brown/red bare soils' are very similar in the global approach (around 0.15 and 0.13, respectively), which could create confusion between these classes. For the local approach, the class centres are better separated (around 0.04 and 0.10 respectively), which probably helps to clear up the confusion. These observations could explain the higher classification performance using the local approach.

Important differences appeared when we compared the percentage of the area of interest classified as 'Buildings' in both approaches (see Table 4). When considering the whole area of interest, 16.80% of the area is classified as 'Buildings' in both approach. This area increases to 17.99% (+1.19%) in the local approach, and to 19.93% (+3.13%) in the global one. The biggest difference between both approaches appears for smaller-sized high and medium density built-up areas.

Table 4: Comparison of the percentage of the area classified as 'Buildings' in both approaches

Morphological Type	Code	Percentage (%) of the map classified as buildings		
		in both approaches	in local approach	in global approach
Non-built-up area	0	0.86	1.3 (+0.44)	1.4 (+0.54)
Small-sized high density built-up fabric	11	24.07	26.04 (+1.97)	29.62 (+5.55)
Small-sized medium density built-up fabric	12	17.86	19.51 (+1.65)	22.51 (+4.65)
Small-sized low density built-up fabric	13	5.86	6.26 (+0.4)	7.35 (+1.49)
Small-sized isolated density built-up fabric	14	2.45	3.01 (+0.56)	3.25 (+0.8)
Medium-sized high density built-up fabric	21	34.84	36.78 (+1.94)	40.33 (+5.49)
Medium-sized medium density built-up fabric	22	20.24	21.49 (+1.25)	23.66 (+3.42)
Medium-sized low density built-up fabric	23	15.78	16.69 (+0.91)	18.57 (+2.79)
Medium-sized isolated density built-up fabric	24	2.1	2.32 (+0.22)	2.77 (+0.67)
Large-sized high density built-up fabric	31	47.76	51.23 (+3.47)	53.02 (+5.26)
Large-sized medium density built-up fabric	32	15.44	16.12 (+0.68)	17.5 (+2.06)
Large-sized isolated density built-up fabric	34	5.17	5.86 (+0.69)	6.22 (+1.05)
	Total	16.8	17.99 (+1.19)	19.93 (+3.13)

The main weakness of the local approach lies in the required processing time which was almost 2.5 times longer than in the global approach. More precisely, the optimization of the segmentation parameter and the segmentation itself required 6.1 hours for the global approach and 15.7 hours for the local one. The processing operations were carried out on a HP® Workstation Z620 equipped with two Intel® Xeon® E5-2680 processors (base frequency at 2.70GHz), both having 8 cores. The optimization step was performed in parallel, using 15 threads. Furthermore, in a context where existing geospatial data to be used as local zones are missing, partitioning the scene into homogeneous local zones proves a very time-consuming task. In this context, future research on local optimization of segmentation parameter could assess the ability to achieve similar results using a regular grid or very large superpixels as local zones for optimization.

The classification results obtained using the local approach are not perfect. Actually, in some situations, the local

This document is the authors version of the paper submitted to Proc. SPIE 10431, Remote Sensing Technologies and Applications in Urban Environments II, ; doi: 10.1117/12.2278422; http://dx.doi.org/10.1117/12.2278422 and available on www.spiedigitallibrary.org

approach failed in classifying correctly some bare-soil objects neighboring buildings whereas the global approach succeeded, as illustrated in Figure 11. However, after meticulous visual assessment, we can affirm that those counter-examples are very rare. Our analysis revealed that, in general, the LULC map produced with a local segmentation parameter optimization approach was more accurate, especially for the class 'Buildings' than that obtained using a global approach. However, more tests should be carried out to verify if that conclusion is consistent when applying the presented framework on different case studies.

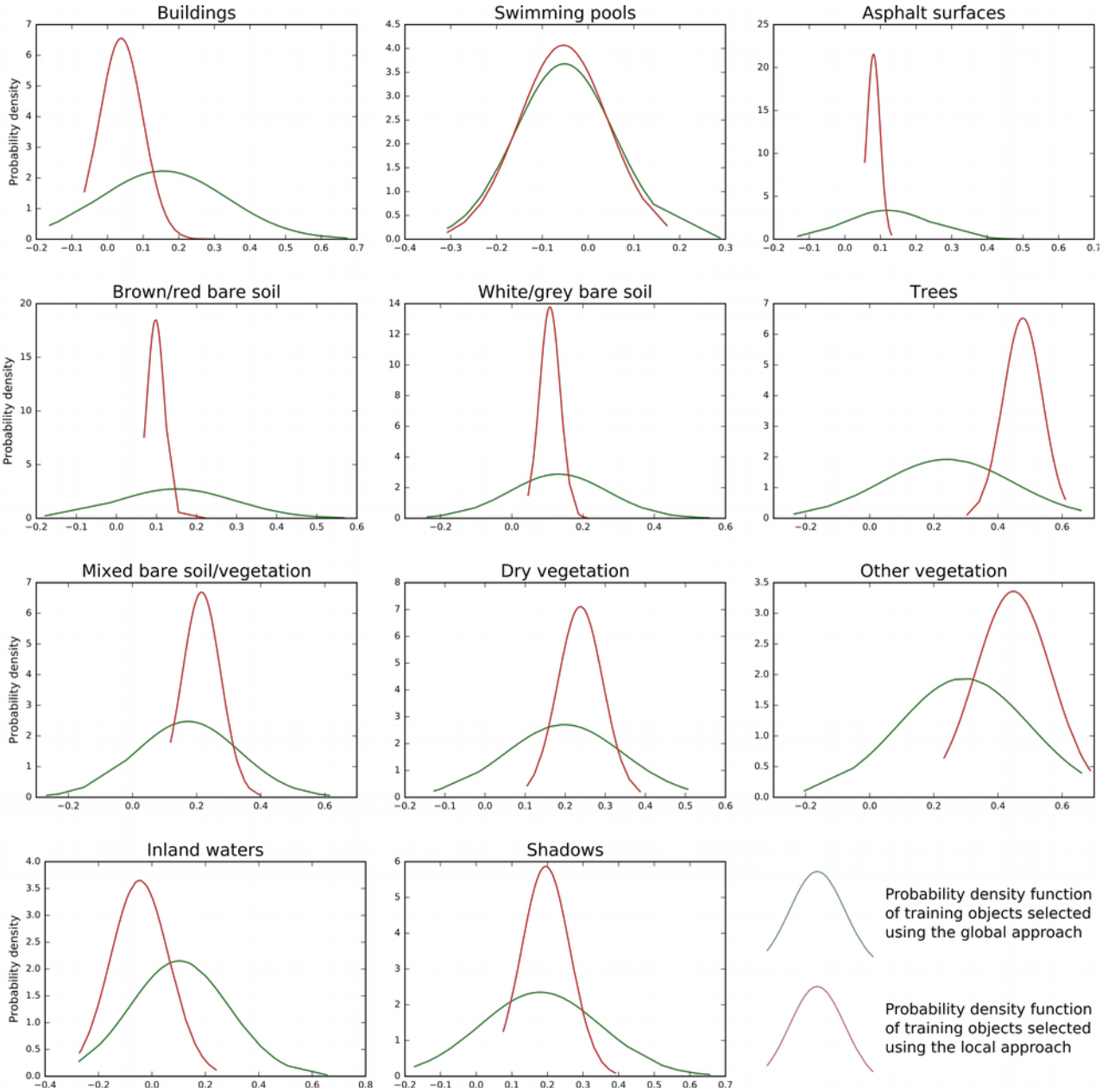

Figure 12: Probability density function of training object statistics for the different classes of the legend. The object feature presented here is the most important variable in the Random Forest classifier, i.e. first quartile on NDVI.

This document is the authors version of the paper submitted to Proc. SPIE 10431, Remote Sensing Technologies and Applications in Urban Environments II, ; doi: 10.1117/12.2278422; http://dx.doi.org/10.1117/12.2278422 and available on www.spiedigitallibrary.org

4. CONCLUSIONS

In this research, we assessed the contribution of a local approach for optimization of segmentation parameters for the production of land-use / land-cover maps in highly heterogeneous urban environments. First, the area of interest was segmented using a global segmentation parameter, which was optimized on a spatial subset representative of the diversity of urban patterns present throughout the whole scene. Then, the optimization of segmentation parameter was carried out for 283 local zones, homogeneous in terms of urban patterns. Both quantitative and qualitative assessments showed that the local approach outperformed the global one. The classification overall accuracy reached 94.77% and 95.45% for the global and the local approach, respectively, using 5 land-cover classes. When considering 11 land-use / land-cover classes, the overall accuracy reached 84.77% and 85.45% respectively. Analysis of training objects features revealed that the local approach helped in improving the separability of different classes. Furthermore, a qualitative assessment of the final maps revealed that the most important improvement of using a local approach resides in the huge reduction of classification errors for bare soils objects neighboring buildings objects, resulting in a better delineation of buildings in the final map. However, this improvement was not reflected by the overall accuracy measures. Therefore, in future work, we will focus on using more targeted methods of assessment. A second possible field of future research is the automation of the delineation of morphological areas, notably based on texture measures, possibly using lower resolution imagery.

ACKNOWLEDGEMENTS

This work was funded by the Belgian Federal Science Policy Office (BELSPO) (Research Program for Earth Observation STEREO III, contract SR/00/304—as part of the MAUPP project—http://maupp.ulb.ac.be). WorldView3 data is copyrighted under the mention "©COPYRIGHT 2015 DigitalGlobe, Inc., Longmont CO USA 80503. DigitalGlobe and the DigitalGlobe logos are trademarks of DigitalGlobe, Inc. The use and/or dissemination of this data and/or of any product in any way derived there from are restricted. Unauthorized use and/or dissemination is prohibited".

REFERENCES

[1] Blaschke, T., "Object based image analysis for remote sensing," ISPRS J. Photogramm. Remote Sens. **65**(1), 2–16 (2010).

[2] Blaschke, T., Hay, G. J., Kelly, M., Lang, S., Hofmann, P., Addink, E., Queiroz Feitosa, R., van der Meer, F., van der Werff, H., van Coillie, F. and Tiede, D., "Geographic Object-Based Image Analysis – Towards a new paradigm," ISPRS J. Photogramm. Remote Sens. **87**, 180–191 (2014).

[3] Gao, Y., Mas, J. F., Kerle, N. and Navarrete Pacheco, J. A., "Optimal region growing segmentation and its effect on classification accuracy," Int. J. Remote Sens. **32**(13), 3747–3763 (2011).

[4] Räsänen, A., Rusanen, A., Kuitunen, M. and Lensu, A., "What makes segmentation good? A case study in boreal forest habitat mapping," Int. J. Remote Sens. **34**(23), 8603–8627 (2013).

[5] Cheng, J., Bo, Y., Zhu, Y. and Ji, X., "A novel method for assessing the segmentation quality of high-spatial resolution remote-sensing images," Int. J. Remote Sens. **35**(10), 3816–3839 (2014).

[6] Yang, J., Li, P. and He, Y., "A multi-band approach to unsupervised scale parameter selection for multi-scale image segmentation," ISPRS J. Photogramm. Remote Sens. **94**, 13–24 (2014).

[7] Zhang, H., Fritts, J. E. and Goldman, S. A., "Image segmentation evaluation: A survey of unsupervised methods," Comput. Vis. Image Underst. **110**(2), 260–280 (2008).

[8] Espindola, G. M., Camara, G., Reis, I. A., Bins, L. S. and Monteiro, A. M., "Parameter selection for region-growing image segmentation algorithms using spatial autocorrelation," Int. J. Remote Sens. **27**(14), 3035–3040 (2006).

This document is the authors version of the paper submitted to Proc. SPIE 10431, Remote Sensing Technologies and Applications in Urban Environments II, ; doi: 10.1117/12.2278422; http://dx.doi.org/10.1117/12.2278422 and available on www.spiedigitallibrary.org

[9] Drăguț, L., Tiede, D. and Levick, S. R., "ESP: a tool to estimate scale parameter for multiresolution image segmentation of remotely sensed data," Int. J. Geogr. Inf. Sci. **24**(6), 859–871 (2010).

[10] Drăguț, L., Csillik, O., Eisank, C. and Tiede, D., "Automated parameterisation for multi-scale image segmentation on multiple layers," ISPRS J. Photogramm. Remote Sens. **88**, 119–127 (2014).

[11] Johnson, B. and Xie, Z., "Unsupervised image segmentation evaluation and refinement using a multi-scale approach," ISPRS J. Photogramm. Remote Sens. **66**(4), 473–483 (2011).

[12] Johnson, B. A., Bragais, M., Endo, I., Magcale-Macandog, D. B. and Macandog, P. B. M., "Image Segmentation Parameter Optimization Considering Within- and Between-Segment Heterogeneity at Multiple Scale Levels: Test Case for Mapping Residential Areas Using Landsat Imagery," ISPRS Int. J. Geo-Inf. **4**(4), 2292–2305 (2015).

[13] Belgiu, M., Drăguț, L. and Strobl, J., "Quantitative evaluation of variations in rule-based classifications of land cover in urban neighbourhoods using WorldView-2 imagery," ISPRS J. Photogramm. Remote Sens. **87**, 205–215 (2014).

[14] Cánovas-García, F. and Alonso-Sarría, F., "A local approach to optimize the scale parameter in multiresolution segmentation for multispectral imagery," Geocarto Int. **30**(8), 937–961 (2015).

[15] Kavzoglu, T., Yildiz Erdemir, M. and Tonbul, H., "A region-based mutli-scale approach for object-based image analysis," ISPRS - Int. Arch. Photogramm. Remote Sens. Spat. Inf. Sci. **XLI-B7**, 241–247 (2016).

[16] Grippa, T., Lennert, M., Beaumont, B., Vanhuysse, S., Stephenne, N. and Wolff, E., "An Open-Source Semi-Automated Processing Chain for Urban Object-Based Classification," Remote Sens. **9**(4), 358 (2017).

[17] Neteler, M., Bowman, M. H., Landa, M. and Metz, M., "GRASS GIS: A multi-purpose open source GIS," Environ. Model. Softw. **31**, 124–130 (2012).

[18] Kluyver, T., Ragan-Kelley, B., Pérez, F., Granger, B., Bussonnier, M., Frederic, J., Kelley, K., Hamrick, J., Grout, J., Corlay, S., Ivanov, P., Avila, D., Abdalla, S., Willing, C. and Jupyter Development Team., "Jupyter Notebooks - a publishing format for reproducible computational workflows," Proc. 20th Int. Conf. Electron. Publ., 87–90, Göttingen, Germany (2016).

[19] McFeeters, S. K., "The use of the Normalized Difference Water Index (NDWI) in the delineation of open water features," Int. J. Remote Sens. **17**(7), 1425–1432 (1996).

[20] Chen, Y., Su, W., Li, J. and Sun, Z., "Hierarchical object oriented classification using very high resolution imagery and LIDAR data over urban areas," Adv. Space Res. **43**(7), 1101–1110 (2009).

[21] United Nations., "World Urbanization Prospects: The 2014 Revision, CD-ROM Edition," United nations, Department of Economic and Social Affairs, Population Division (2014).

[22] Ma, L., Li, M., Ma, X., Cheng, L., Du, P. and Liu, Y., "A review of supervised object-based land-cover image classification," ISPRS J. Photogramm. Remote Sens. **130**, 277–293 (2017).

[23] Belgiu, M. and Drăgut, L., "Comparing supervised and unsupervised multiresolution segmentation approaches for extracting buildings from very high resolution imagery," ISPRS J. Photogramm. Remote Sens. **96**, 67–75 (2014).

[24] Geary, R. C., "The Contiguity Ratio and Statistical Mapping," Inc. Stat. **5**(3), 115 (1954).

[25] Moran, P. A. P., "Notes on Continuous Stochastic Phenomena," Biometrika **37**(1/2), 17 (1950).

[26] Böck, S., Immitzer, M. and Atzberger, C., "On the Objectivity of the Objective Function—Problems with Unsupervised Segmentation Evaluation Based on Global Score and a Possible Remedy," Remote Sens. **9**(8), 769 (2017).

[27] Herold, M., Scepan, J. and Clarke, K. C., "The use of remote sensing and landscape metrics to describe structures and changes in urban land uses," Environ. Plan. A **34**(8), 1443–1458 (2002).

[28] Liu, X., Clarke, K. and Herold, M., "Population density and image texture," Photogramm. Eng. Remote Sens. **72**(2), 187–196 (2006).

[29] Breiman, L., "Random Forests," Mach. Learn. **45**(1), 5–32 (2001).

This document is the authors version of the paper submitted to Proc. SPIE 10431, Remote Sensing Technologies and Applications in Urban Environments II, ; doi: 10.1117/12.2278422; http://dx.doi.org/10.1117/12.2278422 and available on www.spiedigitallibrary.org

[30] McGill, R., Tukey, J. W. and Larsen, W. A., “Variations of Box Plots,” Am. Stat. **32**(1), 12 (1978).